



HAL
open science

Characterization of Turbulence in a Closed Flow

N. Mordant, J.-F. Pinton, F. Chillà

► **To cite this version:**

N. Mordant, J.-F. Pinton, F. Chillà. Characterization of Turbulence in a Closed Flow. Journal de Physique II, 1997, 7 (11), pp.1729-1742. 10.1051/jp2:1997212 . jpa-00248545

HAL Id: jpa-00248545

<https://hal.science/jpa-00248545>

Submitted on 4 Feb 2008

HAL is a multi-disciplinary open access archive for the deposit and dissemination of scientific research documents, whether they are published or not. The documents may come from teaching and research institutions in France or abroad, or from public or private research centers.

L'archive ouverte pluridisciplinaire **HAL**, est destinée au dépôt et à la diffusion de documents scientifiques de niveau recherche, publiés ou non, émanant des établissements d'enseignement et de recherche français ou étrangers, des laboratoires publics ou privés.

Characterization of Turbulence in a Closed Flow

N. Mordant, J.-F. Pinton (*) and F. Chillà

École Normale Supérieure de Lyon (**), 69364 Lyon, France

(Received 29 November 1996, revised 16 June 1997, accepted 16 July 1997)

PACS.47.20.-k – Hydrodynamic stability

PACS.47.27.-i – Turbulent flows, convection and heat transfer

PACS.47.32.-y – Rotational flow and vorticity

Abstract. — We investigate the closed flow between coaxial contra rotating disks, at moderate to high Reynolds numbers. We show that global (*i.e.* spatially averaged) quantities can be used to characterize the state of the flow and its degree of turbulence. We first report measurements on the driving torque and show how it depends on the manner momentum is imparted to the fluid. We then show that pressure measurements at the flow boundary provide a good estimate of the rms velocity fluctuations in the flow and that it reveals the transition to turbulence in the flow volume. Finally, we show that once the transition has occurred, the knowledge of the same global quantities allows the calculation of fundamental turbulence characteristics such as the rms velocity fluctuations, the effective integral length scale L^* , Taylor's microscale λ and Kolmogorov's dissipation length η . That these quantities may be obtained from measuring devices removed from the bulk of the flow is of importance for the study of fluid motion in complex geometries and/or using corrosive fluids.

1. Introduction

The turbulence properties of flows at high Reynolds numbers are usually described experimentally in terms of the scaling properties of the local velocity field, as measured by a small probe placed inside the flow [1–3]. This technique is widely documented and has produced most of the existing experimental data on turbulent flows. Unfortunately the method is complex, local and intrusive; in addition, depending on the flow conditions, it is not always possible to use an anemometer probe *in situ*. Simple examples are flows in which the temperature is very high or not uniform, flows in corrosive liquids, flows in liquid metals [4], *etc.* The question then arises of the experimental characterization of a turbulent flow in the absence of local anemometry measurements. The problem is to determine whether the flow is turbulent and to characterize the intensity of the turbulence, if present. We note that the knowledge of the *integral* Reynolds number is not always sufficient — here *integral* means that it is determined by the values of external parameters fixed in the experiment (for example, the flow rate and tube diameter in a pipe flow). Turbulent flow characteristics may only be determined if one can compute an *internal* turbulent Reynolds number, *i.e.* based on internal flow parameters only. This is the

(*) Author for correspondence (e-mail: pinton@physique.ens-lyon.fr)

(**) CNRS URA 1325

case when local anemometry is available; a turbulent Reynolds number is defined using the rms velocity fluctuations and the Taylor microscale λ . In this article, we justify the use of global measurements to characterize the turbulent fluctuations and we propose alternate ways of defining an *internal* turbulent Reynolds number, at least in the case of a closed flow.

Among possible non-local, non-intrusive measurements are: pressure at the flow boundary, acoustic measurements, power consumption of the flow driving mechanism, *etc.* These measurements are *global* ones, by which term we mean “spatially averaged”:

$$g(t) = \int_{\mathcal{V}} g(\mathbf{x}, t) d^3\mathbf{x}, \quad (1)$$

where the volume \mathcal{V} covers the entire flow or a large part of it. We stress that such a global quantity is an average over space of the instantaneous realization of the flow; it is thus a (fast-varying) function of time whose characteristics — mean value \bar{g} , and fluctuations $\delta g = g(t) - \bar{g}$ — must be studied.

In some cases the scaling of \bar{g} is known in the limit of very high Reynolds numbers. For example, let us consider the case of a disk of radius R rotating at constant angular speed Ω in a fluid of density ρ and kinematic viscosity ν . Dimensional analysis shows that the mean torque required to drive the disks is given by:

$$\bar{\Gamma} = \rho R^5 \Omega^2 f(\text{Re}), \quad (2)$$

where $f(\text{Re})$ is an unknown function of the integral Reynolds number $\text{Re} = R^2 \Omega / \nu$. The functional form of f is itself Reynolds number dependent and varies also with the experiment’s geometry, *e.g.* the surface condition of the disk. Indeed it has been observed that $f(\text{Re}) \sim \text{const.}$, in the limit of very high Reynolds number for (even so slightly) rugose disks [5]. In the case of smooth, highly polished disks, one rather observes a $f(\text{Re}) \sim \text{Re}^\alpha$ behavior. We will return in detail to this point in Section 3.1; for the moment we just stress that f depends on the way the energy is injected into the fluid. The differences in behavior of f come from the fact that the externally fixed parameters (such as Ω) are not simply related to the internal flow variables (such as u_{rms}). The fluid is set into motion *via* its *boundaries* whereas the energetic cost is related to the flow velocity *in the bulk*. It thus can be expected that a more meaningful behavior is recovered when $\bar{\Gamma}$ is expressed in terms of internal flow variables only; *e.g.* $\bar{\Gamma} \sim u_{\text{rms}}^2$. Our point is that such internal quantities can be accessed *via* global measurements that do not require a probe to be inserted into the bulk of the flow; *e.g.* $u_{\text{rms}}[\text{bulk}] \sim \sqrt{p_{\text{rms}}[\text{at wall}]}$.

We describe in the next section our experimental set-up and measurement techniques. We then present our results on torque and pressure measurements, and show how the two measurements can be combined to characterize the transition to turbulence in the flow. We then proceed with the deduction of internal flow parameters (*e.g.* rms velocity fluctuations, energy dissipation, Taylor microscale, *etc.*) and we propose an expression for the turbulent Reynolds number.

2. Experimental Set-Up

2.1. FLOW GEOMETRY. — We use the von Kármán swirling flow [6] produced in the gap between two coaxial counter-rotating disks of radius R , a variable distance H apart. Cylindrical walls surround the flow volume. The experimental set-up is sketched in Figure 1. We use two different fluids, air and water.

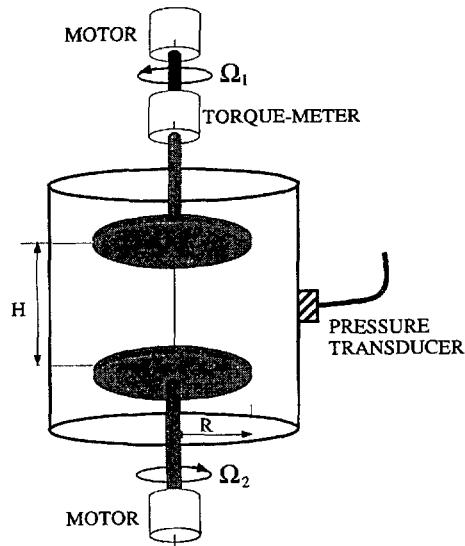


Fig. 1. — Sketch of the experimental set-up in water. The flow is set into motion by the disks counter-rotating at equal frequencies. $H = 20$ cm, $R = 9$ cm. The pressure transducer, mounted flush to the wall, is located in the mid plane between the disks.

- In the case of air, $R = 10$ cm, $H = 40$ cm and the disks are fitted with a set of 8 vertical blades, perpendicular to the disks surfaces, with height $h_b = 2$ cm and thickness 0.5 cm, in order to increase entrainment. The disks are driven by independent 450 watt DC motors, the rotation frequencies of which are adjustable from 0 to 45 Hz and controlled by a feed-back loop. The disks are enclosed in a cylinder 23.2 cm in diameter. The largest Reynolds numbers are thus about $Re = \Omega R^2 / \nu = 10^5$.
- In the case of water, disks of radius $R = 9$ cm, $H = 20$ cm apart, are enclosed in a cylindrical container, 19.3 cm of inner diameter and 19.8 cm in height. Light disks are used in order to reduce inertia effects and thus increase the high frequency cut-off of the torque measurements. The temperature is maintained constant with a regulated water circulation. The disks are rotated independently by two Parvex-Alsthom RS420 motors at controlled rotation frequencies in the range 0–40 Hz. The Reynolds numbers achieved with water are larger than 10^6 . Experiments are performed with disks whose surface is smooth or has a controlled rugosity. Calibrated waterproof sandpaper is used and its rugosity is measured independently with an optical profilometer [7].

We emphasize that in both cases, the forcing of the flow is such that the rotation rate of the disks is kept constant through a feed-back loop. This means that other quantities such as the torque applied by the disks or the energy input are fluctuating quantities in time. An experimental study of these fluctuations has recently been done [8].

2.2. MEASUREMENT TECHNIQUES. — In each case the signal from the transducers are recorded on a National Instruments NBA2150F 16-bits digitizing card which incorporates the necessary anti-aliasing filters.

- Velocity measurements (local) are performed in air using a TSI subminiature hot-film probe with a sensing element $10\ \mu\text{m}$ thick and 1 mm long. Velocities are deduced from voltage measurements using the usual King's law $\sqrt{v} = (e^2 - a)/b$, the validity of which has been checked, and the coefficients a and b obtained from measurements in a calibrated wind tunnel. The position of the probe is adjustable. We have checked that the presence of the probe does not affect the flow measurements by performing identical measurements with the probe support inclined at different angles.
- Pressure measurements in water are done with a 5 mm PCBH112A21 piezoelectric transducer, mounted flush with the lateral wall, in the mid-plane between the disks. It is acceleration-compensated and has a low frequency cut-off at $-3\ \text{dB}$ equal to 50 mHz; its rise-time is 1 ms.
Pressure fluctuations in air are measured by a piezoelectric transducer PCB103A02, also mounted flush with the lateral wall and in the mid-plane. Its active diameter is 2.1 mm, its low frequency cut-off at -5% is 0.05 Hz and its rise-time is $25\ \mu\text{s}$.
- Torque measurements are performed in the experimental apparatus using liquids. One of the disks is connected to the driving motor by a calibrated Lebow torque sensor (strain gage shaft, Model 1102-3.53Nm). Signal-to-noise ratio is improved by the use of an EG&G lock-in amplifier to read the gage bridge output.

3. Results

We first report measurements on the driving torque and show how it depends on the manner with which momentum is imparted to the fluid. We then show that pressure measurements at the flow boundary provide a good estimate of the rms velocity fluctuations in the flow and they permit to recast the torque data onto a very simple form. In particular it reveals the transition to turbulence of the flow.

3.1. TORQUE AND PRESSURE MEASUREMENTS: INTERNAL FLOW VARIABLES. — We measure the torque applied on one of the disks when they rotate in opposite directions at equal rates.

The case of a disk fitted with blades of height h_b is the simplest one: in that situation, the driving torque is just equal to what is needed to set into motion the slices of fluid in between the blades, and a very simple calculation leads to:

$$\bar{\Gamma} \propto \rho R^2 \Omega^2 \frac{h_b}{R},$$

so that referring back to equation (2), $f(\text{Re}) \sim \text{const.}$ and $\bar{\Gamma} \propto \Omega^2$. This is also the case when the entrainment of the fluid is done *via* disks whose rugosity h_b is larger than the boundary viscous sublayer. This is eventually always the case at high rotation rates as observed by many authors [5, 9] and again in Figure 2 (asterisks).

The case of smooth disks is more subtle: the entrainment of the fluid is done through the disks boundary layers and is thus viscosity dependent. The skin friction $\rho\nu(\partial v_{\parallel}/\partial z)$ involves the thickness e of the boundary layer, which decreases as Re increases; in addition its expression depends on whether the flow is laminar or turbulent. In the laminar regime $e \sim \sqrt{\nu/\Omega}$ so that in equation (2) $f(\text{Re}) \sim 1/\sqrt{\text{Re}}$. This has been verified (see [10] for a review), but cannot be observed in our experiment where the rotation rate of the disks is always too high. In the turbulent regime Schlichting's argument using the empirical $\frac{1}{7}$ -th-power velocity distribution law yields a boundary layer thickness $e \sim (\nu/\Omega)^{4/5}$; this gives $f(\text{Re}) \propto \text{Re}^{-1/5}$

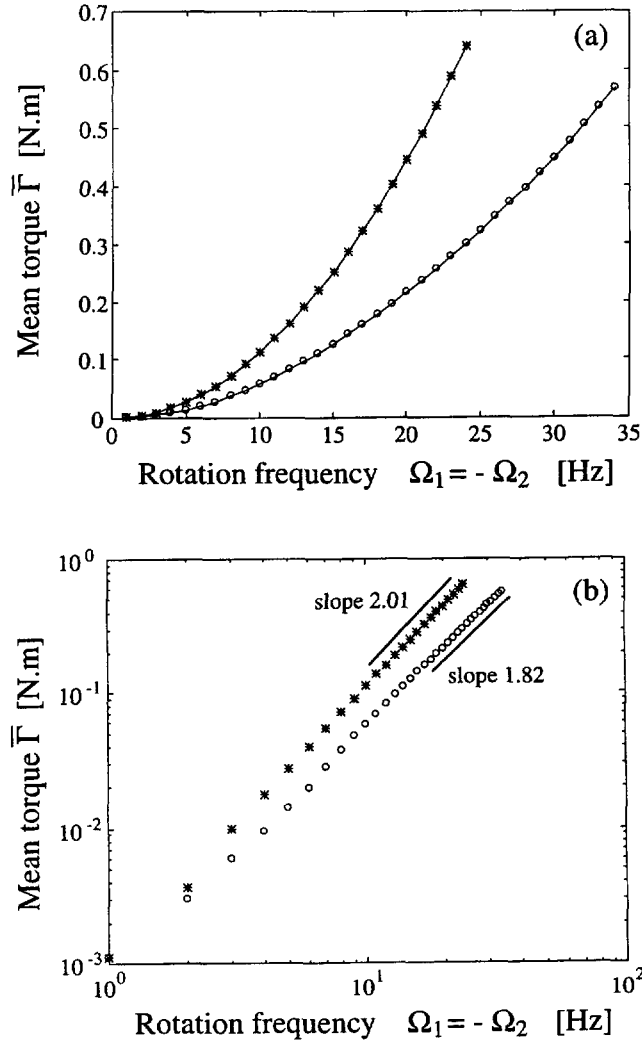


Fig. 2. — Torque measurement in water for disks with varying equal and opposite rotation rates: case of smooth (o) and rugose (*, $\delta = 37 \mu\text{m}$) disks. (a) Linear and (b) logarithmic coordinates.

Our measurements are in agreement with this result; see Figure 2 (circles) where we observe:

$$\bar{\Gamma} \propto \Omega^\alpha \quad \text{i.e.} \quad \frac{\bar{\Gamma}}{\rho R^5 \Omega^2} \propto \text{Re}^{\alpha-2},$$

with $\alpha \sim 1.82$. We thus find $f(\text{Re}) \sim \text{Re}^{-0.18}$.

We note in Figure 2 that these asymptotic scalings are observed in the entire range of explored rotation rates so that the boundary layers are always turbulent. This in turn does not mean that the flow in the gap between the disks is itself turbulent. Indeed the state of the flow depends on many other geometrical characteristics, such as the separation between the disks, the geometry of the container, *etc.* The torque gives only some indication on the forcing of the flow (power input), but the state of the fluid motion can only be obtained from measurements that probe the bulk of the flow.

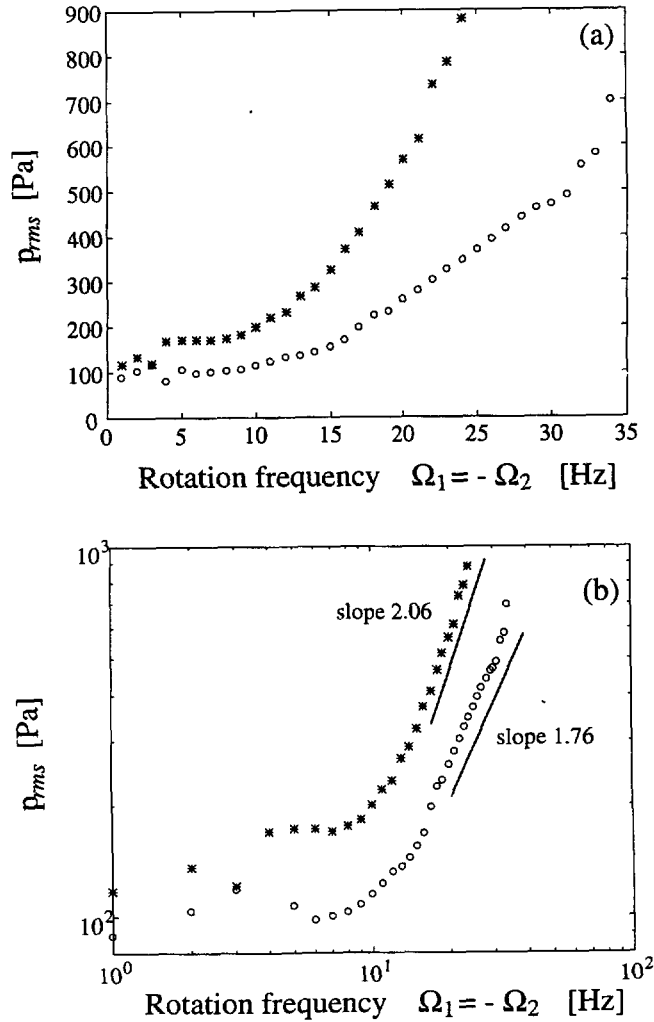


Fig. 3. — Evolution of the variance of the pressure fluctuations in the mid-plane, at the flow wall, in water. In the asymptotic regime $p_{rms} \sim \Omega^2$ for rugose disks (*, $\delta = 37 \mu\text{m}$) and $p_{rms} \sim \Omega^{1.76}$ for smooth disks (o). (a) Linear and (b) logarithmic coordinates.

We now show that the intensity of the velocity fluctuations in bulk can be obtained *via* pressure measurements at the lateral wall, in the mid-plane. We stress that this is a global measurement; just recall that the equation for the pressure:

$$\Delta p = -\rho \nabla \cdot [(\mathbf{u} \nabla) \mathbf{u}] = -\rho \frac{\partial^2 (u_i u_j)}{\partial x_i \partial x_j}, \quad (3)$$

is a Poisson one, the source term of which involves the velocity gradients of the flow (see [11] for an extended review).

Figure 3 shows the evolution of the pressure fluctuation level p_{rms} as the disks rotation rate is varied. It is readily observed that, contrary to torque measurements, the pressure fluctuations

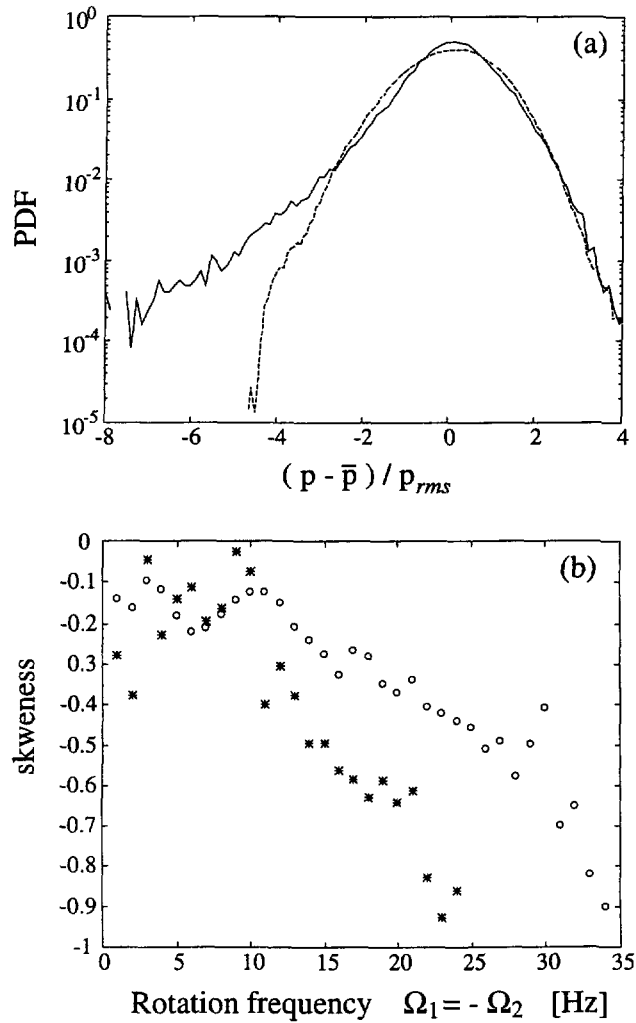


Fig. 4. — Evolution of the Probability Density Function of the pressure fluctuations. Measurement in water, at the wall in the mid-plane. (a) Comparison of low rotation rate (dotted line, $\Omega = 2$ Hz) and high rotation rate (solid line, $\Omega = 34$ Hz). (b) Comparison of the variation of the PDFs' skewness with the disks rotation frequency; (o): smooth disks and (*): disks with $\delta = 37 \mu\text{m}$ rugosity.

display a change of behavior when going from slow to fast disk rotation. At low Ω , p_{rms} remains at an almost constant level, while in the limit of large rotation rates it scales asymptotically as a power law, as expected in a turbulent flow [12,13]. Note, however that once again the scaling depends on the entrainment mechanism, as illustrated by the difference of behavior between smooth and rugose disks.

This change of behavior is also visible on the Probability Density Functions (PDFs) of the pressure fluctuations (see Fig. 4a): at low Ω the PDFs are Gaussian, while in the turbulent regime they display the well known exponential tails towards low values [14]. This change of behavior in the PDFs shape may be measured by its skewness (see Fig. 4b). At low rotation rates, the skewness remains about constant while it decreases almost linearly in the turbulent regime. We note that the transition seems to be more abrupt when rugose disks are being used.

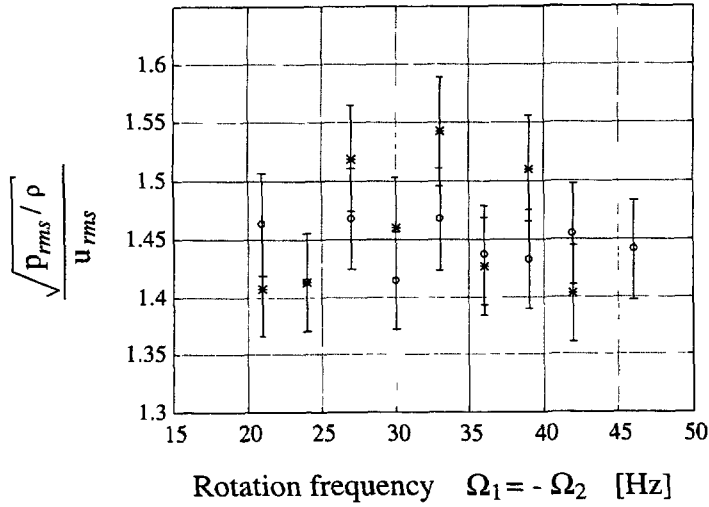


Fig. 5. — Velocity rms fluctuations in air (disks fitted with blades) calculated from pressure fluctuations at the lateral wall compared to the measurements using hotwire anemometry (both scaled in m/s). (o): pressure measured at $h = 5$ cm above the lower disk and velocity recorded at the same height, at $r = 5$ cm from the axis. (*): $h = 11$ cm and $r = 3$ cm.

We thus observe that the pressure at the flow wall reveals the transition of the flow to a turbulent state. We now show that p_{rms} yields a meaningful measurement of the variance of the velocity fluctuations, u_{rms} , in the bulk of the flow. On dimensional grounds, one expects $p_{rms} = \rho u_{rms}^2 g(\text{Re})$ where $g(\text{Re})$ is an arbitrary function of the Reynolds number. In the turbulent regime, the simplest case is $g(\text{Re}) \rightarrow \text{const.}$ as $\text{Re} \rightarrow \infty$, so that $p_{rms} \propto \rho u_{rms}^2$. It has been shown to be the case in the quasi-Gaussian approximation [15,16], so that the pressure fluctuations are mostly governed by the velocity fluctuations at the integral scale although the source term in its equation involves the velocity gradients.

We have directly tested the proportionality of u_{rms}^2 and p_{rms} in the experimental set-up in air, where simultaneous pressure and velocity measurements are possible. Velocity measurements are made using hotwire anemometry, at different radial and vertical positions within the flow. We obtain $u_{rms} = (0.22 \pm 0.03)u_{\text{disk}}$ throughout the measurement volume, where $u_{\text{disk}} = 2\pi R\Omega$ is the disk rim velocity. On the other hand, we observe $\sqrt{p_{rms}/\rho} = (0.32 \pm 0.02)u_{\text{disk}}$ when the pressure is recorded at the wall either in the center of the measurement volume or nearer to one of the disks. Altogether, it gives $\sqrt{p_{rms}/\rho} = (1.45 \pm 0.07)u_{rms}$, independent of the locations of the anemometer probe and of the pressure transducers, for all disks rotation frequencies (see Fig. 5).

We then reconsider our torque measurements using $\sqrt{p_{rms}/\rho}$ (instead of $R\Omega$) as a characteristic velocity scale (an approach already used in [17]). The behavior is radically changed as shown in Figure 6, where we have plotted $\bar{\Gamma}/\mathcal{V}p_{rms}$ vs. $\sqrt{p_{rms}}$ (\mathcal{V} is the volume of fluid in motion).

- (i) a sharp transition can be observed at a critical value p_{rms}^* , giving evidence for a clear transition in the flow, which becomes turbulent when the velocity fluctuations exceed a certain threshold.
- (ii) for values of the rotation rate such that $p_{rms} > p_{rms}^*$, the torque scales as p_{rms} . This scaling range is verified as soon as the entire flow becomes turbulent.

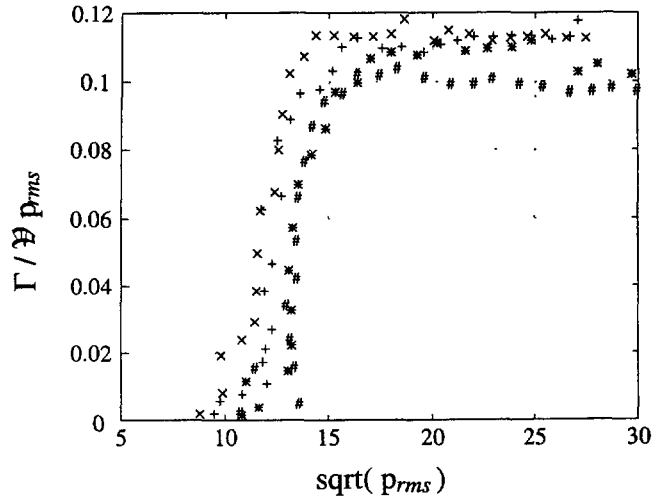


Fig. 6. — Variation of the torque applied on one disk with intensity of velocity fluctuations in the flow, as measured by $\sqrt{p_{rms}}$. The torque is adimensionalized by $\mathcal{V} p_{rms}$, where \mathcal{V} is the volume of the fluid. Measurements for various disks rugosities: (+) 8.6 μm , (x) 11.3 μm , (#) 23.7 μm , (*) 37 μm .

Note that all curves (with smooth or rugose disks) collapse on the same shape, showing the very simple behavior of the driving torque when recast in term of internal flow variables alone; it allows a determination of the transition of the flow to a turbulent state (of course the threshold is not universal, it depends on the geometry of the experiment) and gives the appropriate scaling for the global measurements performed on the flow.

3.2. TURBULENCE CHARACTERISTICS. — The torque, rotation rate and pressure fluctuations give access to two fundamental quantities: the power input ($P = \Gamma \cdot \Omega$, characteristic of the forcing intensity) and the amplitude of the velocity fluctuations ($\sqrt{p_{rms}/\rho}$, characteristic of the response of the fluid). These quantities allow the calculation of the characteristic length scales of the turbulent motion: the integral length scale L^* of the flow, Taylor microscale λ and the Kolmogorov dissipation length η .

3.2.1. *Integral Scale L^** . — In most experiments L^* is identified with a characteristic scale L of the experimental set-up (e.g. the grid mesh size in grid-turbulence). It is a fixed parameter, independent of the forcing of the flow, even though its physical meaning is to give the size of the energy containing eddies. Its evaluation is made more precise in numerical studies which define it through the velocity power spectrum:

$$\frac{2\pi}{L^*} \sim \frac{\int k E(k) dk}{\int E(k) dk}$$

We propose to keep the spirit of this definition and to calculate L^* as a characteristic size of the energy input into the flow. Equating the power consumption of the flow to the rate of change of the kinetic energy of structures of size L^* , one obtains:

$$\frac{\bar{P}}{\rho \mathcal{V}} \sim \frac{u_{rms}^3}{L^*} \Rightarrow L^* \sim \frac{\rho \mathcal{V} \left(\frac{p_{rms}}{\rho} \right)^{3/2}}{\bar{P}}. \quad (4)$$

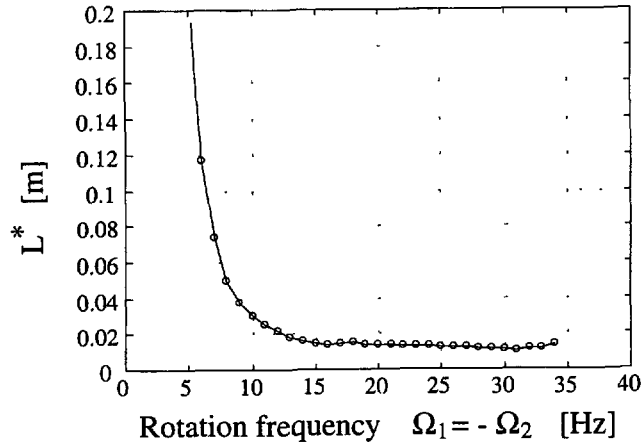


Fig. 7. — Measurement with smooth disks. Integral length scale L^* , calculated from the energy consumption of the flow and the pressure fluctuations at the boundary.

The variation of L^* with the disks rotation frequency is displayed in Figure 7. It decreases rapidly from the height of the fluid (20 cm) at low rotation rates to about 2 cm at the transition to turbulence. Above the threshold, it remains constant to that value. We note that in the turbulent regime L^* is 10 times smaller than the diameter of the disks and that it does not correspond to any particular length in the experimental set-up. This confirms the need to calculate it from flow measurements.

3.2.2. Taylor Microscale λ . — This is the scale characteristic of the maximum of enstrophy. Its measurement gives the inner length scale of the turbulent motion. Together with u_{rms} it yields a Reynolds number R_λ which characterizes the intensity of the turbulence, independently of the experimental arrangement. In addition, it has been proposed [17, 18] that λ is the characteristic length scale of the vorticity filaments observed in swirling flows. Traditionally, the Taylor microscale is obtained from local hotwire anemometry, using:

$$\frac{1}{\lambda^2} \sim \frac{1}{u_{\text{rms}}^2} \overline{(\nabla \mathbf{u})^2},$$

and in the present computation, the Taylor hypothesis is used to relate time measurements at a fixed location to the spatial velocity profile [19–21]. We propose to retain the above definition of λ , but to estimate the velocity gradients from the dissipation, equating the time averaged power input and the viscous dissipation rate:

$$\frac{\overline{P}}{\rho \mathcal{V}} \sim \nu \overline{(\nabla \mathbf{u})^2} \quad \text{i.e.} \quad \lambda^2 \sim \nu \frac{u_{\text{rms}}^2}{\overline{P}/\rho \mathcal{V}} = \nu \frac{p_{\text{rms}}}{\overline{P}/\mathcal{V}} \quad (5)$$

The numerical values — see Figure 8a are close to the one directly obtained in similar conditions from ultrasound scattering measurements of the filaments core size [17]. Figure 8b shows the corresponding turbulent Reynolds number $R_\lambda = u_{\text{rms}}\lambda/\nu$; one observes that the values are comparable to the one measured from local anemometry and that the usual asymptotic behavior $R_\lambda \sim \sqrt{\text{Re}}$ is observed in the turbulent regime.

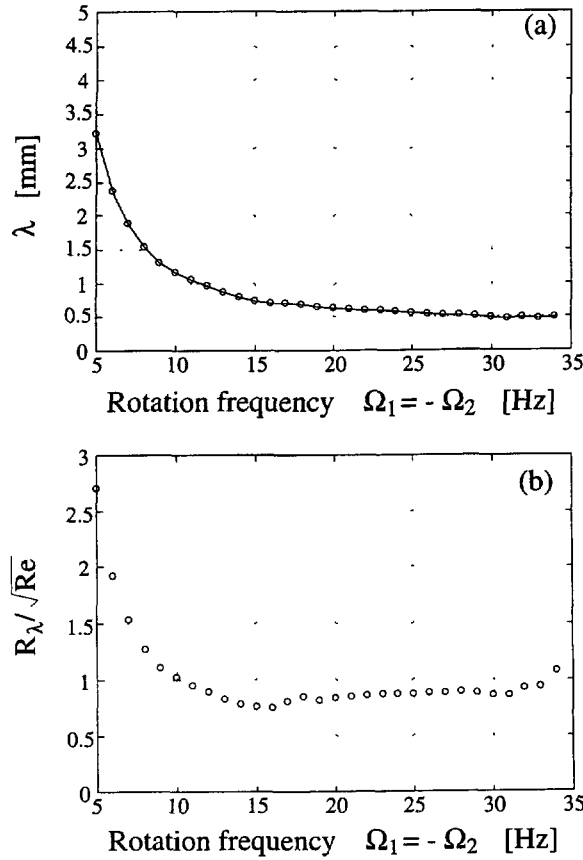


Fig. 8. — Measurements with smooth disks. (a) Calculation of the Taylor microscale from the rms velocity fluctuations and energy dissipation in the flow. (b) Evolution of the Taylor-based turbulent Reynolds number $R_\lambda = u_{rms}\lambda/\nu$ with the integral (experimental) Reynolds number $Re = R^2\Omega/\nu$. In the turbulent regime $R_\lambda \propto \sqrt{Re}$, as expected.

3.2.3. *Kolmogorov Dissipation Length η .* — This scale is characteristic of the viscous friction, *i.e.* of the transfer of the kinetic energy of the turbulent motion to heat. It gives the size of the smallest possible structures in the flow. In the turbulent regime it is estimated from the power consumption of the flow:

$$\eta \sim \left(\frac{\nu^3}{\overline{P}/\rho\nu} \right)^{1/4} \tag{6}$$

The variations of η with the disks rotation frequency are shown in Figure 9a. In the turbulent regime, one recovers the usual relationship $\frac{\eta}{L^*} \sim Re^{3/4}$, as observed in Figure 9b.

3.2.4. *Comparison with Hot-Wire Measurements.* — To establish further the calculation of turbulence small scales characteristics from global measurements, we have compared the results with traditional hot-wire anemometry, in the setup using air as the working fluid. The dissipation is estimated from the local velocity measurements as $\epsilon_L \sim C_\epsilon \nu < (\partial u / \partial x)^2 >$, where u is the local flow velocity and a localized Taylor hypothesis [21] is used to relate temporal and

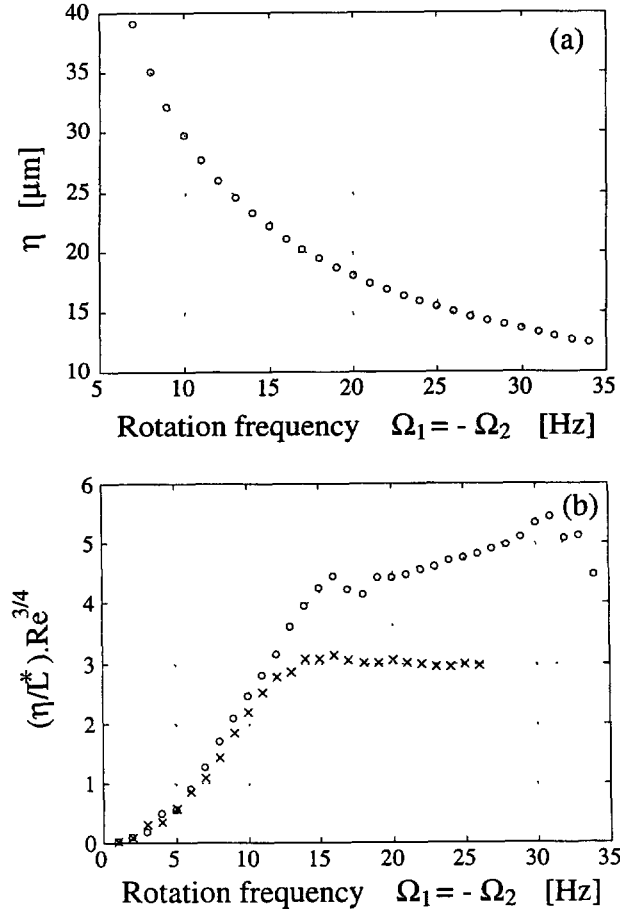


Fig. 9. — Measurement with smooth disks. (a) Kolmogorov dissipation length η , calculated from the energy input in the flow. (b) Scaling of η with the integral length scale L^* , as a function of the integral (experimental) Reynolds number $\text{Re} = R^2\Omega/\nu$. In the turbulent regime $\eta \propto L^*\text{Re}^{-3/4}$

spatial derivatives. The constant C_ϵ is considered to be equal to 15 since the velocity u is measured near center of the gap between the disks, where the flow is expected to be homogeneous. The dissipation is also calculated from the motors power consumption as $\epsilon_G = (P_{\text{mechanical}})/M$.

Kolmogorov's dissipation scale is then calculated as $\eta_{G,L} = (\nu^3/\epsilon_{G,L})^{1/4}$ for several values of the disk rotation frequencies. The results, displayed in Figure 10, show that both methods yield the correct order of magnitude for η . However, the Reynolds number dependence $\eta \sim L\text{Re}^{-3/4}$ is only observed for the global measurements. It shows that it is very difficult to obtain a good estimate of ϵ_L using local velocimetry in closed flows where the velocity fluctuation level is very high (about 35% here). We have tried other alternatives for the calculation of ϵ_L , such as using the Karman-Howarth relationship, again the order of magnitude is correct, but not the Reynolds number dependence. It also affects the measurements of the Taylor microscale λ when it is estimated from the local velocity measurements: the order of magnitude is the same as when derived from the mechanical power input in the flow, but it does not exhibit the expected $\lambda \sim \text{Re}^{-1/2}$ scaling.

We thus observe that the global measurements yield a correct and coherent estimation of the turbulence small scale characteristics in a closed flow.

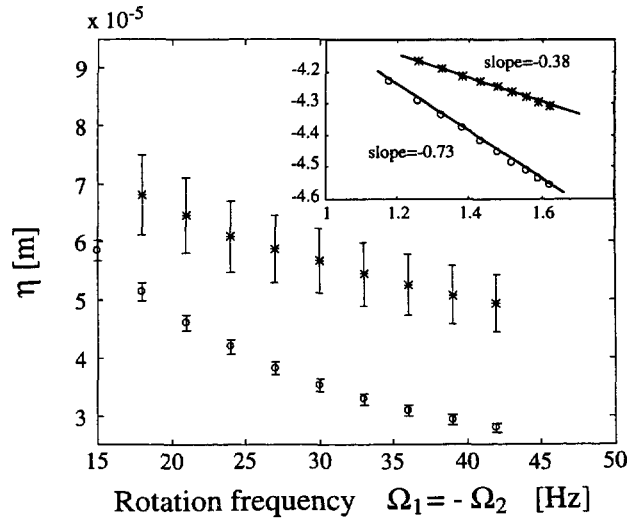


Fig. 10. — Calculation of Kolmogorov dissipation length, from power consumption and pressure fluctuations (\circ), and from local hotwire measurements ($*$) — probe position $h = 11$ cm, $r = 3$ cm. The inset shows the data in logarithmic coordinates.

4. Conclusion

We have shown here that it is possible to investigate the dynamical behavior of a closed flow at moderate to high Reynolds numbers using global (*i.e.* spatially averaged) measurements only. These measurements are very simple and do not require that sophisticated probes be introduced in the bulk of the flow. The scaling of relevant physical quantities such as the applied torque or power consumption in terms of internal flow variables (*e.g.* u_{rms}) reveals the transition to the turbulent regime. It does so much more clearly than the corresponding variations with the experimental control parameters (*e.g.* disks rotation rate). Furthermore, once the transition has occurred, the turbulence can be characterized with the knowledge of the same global quantities. Indeed, the measurements of the power input and of pressure fluctuations at the wall are sufficient to calculate fundamental turbulence characteristics such as the rms velocity fluctuations or the typical length scales L^* , λ and η . Then $[L^*, \eta]$ is the interval of motion sizes in the flow, of L^*/λ yields an estimate of the inertial range, while R_λ measures the overall intensity of the turbulence. That these quantities may be obtained from measuring devices removed from the bulk of the flow is of importance for the study of fluid motion in complex geometries and/or using corrosive fluids.

Acknowledgments

We acknowledge helpful discussions with Stephan Fauve. Many thanks to Sergio Ciliberto who assisted us in the measurement of the sand paper rugosity with his optical profilometer. The experimental set-up could not have been modified so many times without the (patient) expertise of Marc Moulin and Franck Vittoz.

References

- [1] Tennekes H. and Lumley J.L., A first course in turbulence (The MIT Press, 1971).
- [2] Nelkin M., *Adv. Phys.* **43** (1994) 143-181.
- [3] Frish U., Turbulence (Cambridge U. Press. 1995).
- [4] Magnetohydrodynamics flows are of importance in a wide range of areas, ranging from the study of heat transfers in nuclear reactors cooling circuits to the understanding of the dynamo effect that generates the magnetic field of planets.
- [5] Nagata S., Mixing, chap.1, (J. Wiley & Sons, 1975).
- [6] For reviews on these so-called "von Karman swirling flows", see for instance, Zandbergen P.J. and Dijkstra D., *Ann. Rev. Fluid Mech.* **19** (1987) 465-491.
- [7] Arecchi F.T., Bertani D. and Ciliberto S., *Opt. Commun.* **31** (1979) 263.
- [8] Labbé R., Pinton J.-F. and Fauve S., *J. Phys II France* **6** (1996) 1099-1100.
- [9] Labbé R., Pinton J.-F. and Fauve S., *Phys. Fluids* **8** (1996) 914-922.
- [10] Schlichting H., Boundary-layer theory (McGraw-Hill, 1979).
- [11] Fauve S., Abry P., Derroncourt B., Labbé R. and Pinton J.-F., to appear in Non Linear Science Today, Behringer, Ed. (Springer-Verlag, 1996).
- [12] Abry P., Fauve S., Flandrin P. and Laroche C., *J. Phys. II France* **4** (1994) 725-733.
- [13] Cadot O., Douady S. and Couder Y., *Phys. Fluids* **7** (1995) 630-646.
- [14] Fauve S., Laroche C. and Castaing B., *J. Phys. II France* **3** (1993) 271-278.
- [15] Batchelor G.K., *Proc. Cambridge Phil. Soc.* **47** (1951) 359-374.
- [16] George W.K., Beuther P.D. and Arndt R.E.A., *J. Fluid Mech.* **148** (1984) 155-191.
- [17] Derroncourt B., Pinton J.-F. and Fauve S., submitted to *Physica D*.
- [18] Hernandez R. and Baudet C., in Proceedings of the Vth European Turbulence Conference, Kluwer, (1996).
- [19] Taylor G.I., *Proc. Roy. Soc. A.* **164** (1928) 476.
- [20] Fisher M.J. and Davies P.O.A.L., *J. Fluid Mech.* **18** (1964) 97-116.
- [21] Pinton J.F. and Labbé, R., *J. Phys. II France* **4** (1994) 1461-1468.